Steady-State and Dynamic Fluorescence Measurements of a Perylene-Labeled Triblock Copolymer: Evidence for Ground-State Dye Aggregate Formation

Matthew Moffitt, J. P. S. Farinha, and M. A. Winnik*

Department of Chemistry, University of Toronto, 80 St. George Street, Toronto, Ontario, Canada M5S 3H6

Ulrike Rohr and Klaus Müllen*

Max-Planck-Institut für Polymerforschung, Ackermannweg 10, D-6500 Mainz, Germany

Received March 4, 1999; Revised Manuscript Received May 19, 1999

ABSTRACT: Steady-state fluorescence and fluorescence decay measurements were carried out on a perylene-labeled triblock copolymer, polystyrene-*b*-poly(ethylene-*co*-butylene)-*b*-polystyrene (SEBS), both in toluene solution and in a thin film. For the polymer solution, the data fit well to a double-exponential function, and the same two lifetimes $\tau_{short} = 4.4$ ns and $\tau_{long} = 9.2$ ns, but with different relative intensities, are recovered at different emission wavelengths. The longer lifetime, $\tau_{long} = 9.2$ ns, is attributed to the presence of dye aggregates, with $\tau_{short} = 4.4$ ns assigned to unassociated dye. This interpretation of decay profiles is supported by steady-state fluorescence measurements: the onset of aggregate emission corresponds to a sharp decrease in the ratio of preexponential factors, A_{short}/A_{long}. Excitation spectra of the labeled polymer are found to be dependent on the emission wavelength, suggesting that the population of aggregated dye molecules exists in the ground state prior to excitation. The fractional contribution of unimer fluorescence in the polymer film ($f_{short} = 0.36-0.10$) is much smaller than that in solution ($f_{short} = 0.97-0.84$), suggesting a higher degree of aggregate formation in the film.

Introduction

The thermal and photochemical stability of perylene and its derivatives, together with their photoactive and possible photoconductive properties, make this class of π-conjugated organic chromophores attractive candidates for a number of industrial applications. Some of the more common uses of perylene dyes include coloration or marking of plastics and textiles,[1] dyes for lasers,[2,3] liquid crystal displays,[4] solar cells,[5] and dyes for photographic and reproduction processes.[6] For more specialized applications, such as the development of organic light-emitting diodes (LED's)[7] or nonlinear optical devices,[6] the incorporation of perylene dyes into a suitable polymer matrix becomes an important issue and opens the door to soluble, processable materials that can be cast as thin films or molded into different forms. Fundamental studies of morphology in polymer blends would also benefit from the incorporation of perylene dyes into polymer systems. In laser scanning confocal fluorescence microscopy (LSCFM) experiments, for example, the dyes would serve as extremely efficient fluorescent labels, due to their high quantum yields and resistance to photobleaching. As well, the red-orange color of most perylene dyes is well suited to the wavelengths of Ar ion lasers, commonly used in LSCFM experiments. More subtle experiments, involving perylene dyes in energy-transfer (ET) pairs, can also be imagined, in which the labels would act as molecular-level probes in studies of polymer interfaces. The relatively high absorption and emission wavelengths of perylene dyes would be a definite advantage in this area, as absorption and emission from impurities are often found to overlap with the spectra of traditional donor−acceptor pairs such as phenanthrene−anthracene.

A number of polymers have been synthesized in which perylene is directly incorporated into the backbone, in the form of partially fused polyperylene[8] or perylene-containing polyimides.[9−12] Due to the rigidity of the perylene moieties, and the low solubility of polyimides, the development of soluble and processable materials of this type has led to certain synthetic challenges.[12]

In the present paper, we introduce a new type of perylene-containing polymer, in which an extremely low concentration of chromophores is joined to the main chain via a simple post-polymerization reaction. The starting polymer is a triblock copolymer, polystyrene-*b*-poly(ethylene-*co*-butylene)-*b*-polystyrene (SEBS, Shell), in which the olefin block has been lightly maleated. Reaction with the perylene derivative **1** (Chart 1) produces a perylene-labeled SEBS copolymer, with dye molecules joined to the middle EB block. Since both blocks of the copolymer are noncrystalline and completely soluble in a number of organic solvents, it is possible to cast thin, transparent films of the labeled material, facilitating fluorescence measurements in solution and the solid state and providing an example of a processable material incorporating perylene dyes. Using the same approach, perylene chromophores could be attached to a wide range of maleated polymers. The concentration of perylene groups is stoichiometrically controlled and is independent of the polymerization reaction.

A traditional problem in the industrial application of perylene dyes is their tendency to aggregate into high-melting crystals that are difficult to process. In the design and synthesis of the perylene derivative **1**, substituents are used to disrupt packing in the crystalline state of the dye: the 2,6-diisopropylphenylimide substituent is twisted approximately perpendicular to

* To whom correspondence should be addressed.

10.1021/ma990332s CCC: $18.00
Published on Web 07/08/1999

Chart 1

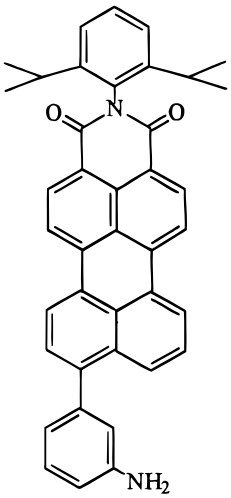

1

the perylene face, as is the 3-aminophenyl group attached to the 9-position of the perylene. Although these substituents may prevent the formation of well-packed crystals, we shall see that this strategy does not eliminate the potential for aggregate formation.

It is well-known that certain dyes have a tendency to aggregate under various conditions, forming dimers or larger assemblies with spectroscopic properties that are distinct from those of the monomer; dye aggregation in aqueous[13] and nonaqueous[14] solutions, surfactant colloids,[15] Langmuir−Blodgett films,[16] sol−gel matrices,[17] and metal oxide colloids[18] have been previously reported. In particular, the aggregation of perylene dyes has been investigated in several systems[13h,15b,c,6d,19] and has been found to result in aggregates with a range of photophysical properties, including excimers[16d] and nonfluorescent dimers.[13h]

The study of dye aggregation in polymer films has been motivated, in part, by reported nonlinear optical responses in polymer/dye composites and by the potential commercial applications of these materials in the area of integrated optics.[20,21d] Of particular interest are the enhanced photoconductivity and photoluminescence properties of certain dye assemblies, such as the red-shifted J-aggregates of cyanine and other dyes.[13a] Due to the dependence of optical properties on the size and structure of dye aggregates, the ability to control dye aggregation in polymer films is a desired goal.

Most of the previous work on dye aggregation in polymer films has involved "free" dye molecules dispersed in a polymer matrix;[20,21] in such systems, the extent of dye aggregation is essentially limited by the molecular architecture of the dye and the kinetics of dye diffusion through the film. A very different situation arises when dye molecules are covalently attached to the polymer chain as "tags" or "labels" or directly incorporated into the backbone, as in the case of perylene-containing polyimides. In these systems, the mobility of the dye over certain length scales is ultimately limited by the mobility of the polymer chains in solution or in thin films. In a solution study of a perylene-containing polyimide, the presence of dye aggregates was attributed to chain coiling in the organic solvent.[19] Such dependence of dye aggregation on chain mobility and conformation may provide an invaluable key to studies of other phenomena related to localized changes in polymer concentration, including micellization and polymer adsorption. However, certain experiments on dye-labeled polymers, such as those involving energy transfer between donor and acceptor dyes, would be greatly impeded by the formation of aggregates. Clearly, an understanding of dye aggregation under different conditions, and a knowledge of the spectroscopic properties of the aggregates, are crucial to the design of useful experiments involving dye-labeled polymers.

The present work details the chemical and spectroscopic characterization of the SEBS copolymer labeled with perylene dye **1**. A combination of fluorescence spectroscopy (steady-state measurements) and fluorescence decay profiles (dynamic measurements) provide intriguing evidence for the existence of ground-state dye aggregates, both in solution and in the solid state. Decay times are determined for aggregate and unimer populations, and the contributions of the aggregates to fluorescent emission in solution and in the solid state are compared. Although the physical origin of dye aggregates in this system is not entirely understood, they are attributed to local concentration effects in solutions and films of the labeled polymer.

Experimental Section

Synthesis of Aminoperylenemonoimide. The perylene derivative **1** ((*N*-(2,6-diisopropylphenyl)-9-(3-aminophenyl)-perylene-3,4-dicarboximide), Chart 1) was synthesized in the following manner. One gram (1.8 mmol) of *n*-(2,6-diisopropylphenyl)-9-bromoperylene-3,4-dicarboximide,[22] 360 mg (2.3 mmol) of 3-aminophenylboronic acid (Aldrich), and 180 mg (0.16 mmol, 9 mol %) of $Pd(PPh_3)_4$ were dissolved in 100 mL of toluene and 20 mL of 2 N K_2CO_3. The reaction mixture was stirred at 120 °C for 12 h. The solution was then poured into 200 mL of diluted HCl and extracted with CH_2Cl_2. The organic layer was dried over $MgSO_4$, followed by evaporation of the solvent. The crude product was purified by column chromatography, using a silica gel substrate and a 3:1 (v/v) mixture of petroleum ether/CH_2Cl_2 as an eluent. A total of 700 mg (yield = 68%) of the red product (mp = 232 °C) was isolated. The product in deuterated chloroform yielded the following ^{1}H (500 MHz) and ^{13}C (125 MHz) NMR data, corresponding to structure **1**:

^{1}*H NMR Spectrum:* δ = 8.63−8.58 (2 d, ^3J = 8.2 Hz, 2H), 8.47−8.38 (m, 4H), 8.07−8.05 (d, ^3J = 8 Hz, 1H), 7.59−7.55 (m, 2H), 7.54−7.49 (t, ^3J = 8 Hz, 1H), 7.54−7.48 (t, ^3J = 7.8 Hz, 1H), 7.37−7.35 (d, ^3J = 7.8 Hz, 2H), 7.28−7.25 (dd, $^3J_1$ = $^3J_2$ = 7.9 Hz, 1H), 6.90−6.88 (d, $^3J_1$ = 7.9 Hz, 1H), 6.85 (s, 1H), 6.82−6.80 (d, ^3J = 7.9 Hz, 1H), 2.83−2.74 (hept, ^3J = 6.8 Hz, 2H), 1.17−1.15 (d, ^3J = 6.8 Hz, 12H).

^{13}*C NMR Spectrum:* δ = 164.52 (C=O), 147.44, 146.59, 144.31, 141.32, 138.31, 138.09, 134.01, 132.30, 132.26, 132.03, 131.02, 130.13, 129.79, 129.66, 129.60, 129.58, 128.79, 128.75, 128.42, 127.32, 127.28, 124.51, 124.39, 124.15, 121.35, 121.29, 120.78, 120.50, 120.44, 116.75, 114.81, 29.50 (CH(CH_3)$_2$), 24.11 (CH(CH_3)$_2$).

The FD mass spectrum (8 kV) of dye **1** reveals a single base peak, attributed to the molecular ion, with m/z = 572.0; this agrees well with the predicted molecular weight value of 572.7 g/mol for the compound. The melting point of the purified dye was found to be 232 °C.

Analysis of FT-IR data for the dye also agrees well with the structure shown above. Principal peaks of the FT-IR spectrum for the dye on KBr are as follows: ν (cm^{-1}) = 3050, 2961, 2929, 2926, 2867, 1696, 1654, 1590, 1571, 1359, 1291, 1244, 1196, 1178, 840, 833, 811, 791, 784, 764, 755, 747, 706.

Labeling of SEBS Copolymer with Aminoperylenemonoimide. The maleated "Kraton" triblock copolymer, polystyrene-*b*-poly(ethylene-*co*-butylene)-*b*-polystyrene (SEBS),

was obtained from Shell with the following specifications: weight ratios S:EB:S = 1:5:1, M_w = 97 700, M_n = 84 400, M_w/M_n = 1.15; the polymer had been maleated with 2 wt % maleic anhydride. A 2 g sample of the polymer was dissolved in 400 mL of *o*-xylene at 150 °C. Eleven milligrams (0.02 mmol) of the perylene derivative **1** and 120 mg of acetic acid were added. The reaction mixture was stirred at 150 °C for 12 h. The temperature was then lowered to 130 °C, and 500 mg (4.95 mmol) of hexylamine was added to react with remaining anhydride functionalities. The mixture was stirred at 130 °C for another 12 h. The polymer was precipitated into 1.5 L of acetone and recovered by filtration. The precipitation procedure was repeated several times, until the acetone solution was colorless; this ensured that all unreacted perylene derivative was removed from the sample. Following the final filtration step, the polymer was dried under vacuum at room temperature. A 1.9 g sample of the salmon-colored polymer was isolated (yield = 95%).

Characterization of Perylene-Labeled SEBS: FTIR, GPC, and UV−vis Measurements. Fourier transform infrared (FTIR) spectra of the labeled and unlabeled SEBS copolymer were obtained using a Perkin-Elmer Spectrum 1000 spectrometer. Both samples were cast onto the hydrophilically modified surface of a PTFE film from CCl_4 solutions and heated under vacuum at 120 °C for 2 h; this procedure converts any remaining carboxylic acid functionalities, which can form during storage under ambient conditions, back into succinic anhydride groups. The dried films were then removed from the PTFE substrate and attached to KBr windows for data collection.

Gel-permeation chromatography (GPC) of the labeled polymer was carried out on a Waters 515 instrument, equipped with a Waters 410 differential refractometer (refractive index detector) and a Kratos fluorescence detector. The perylene-labeled polymer was dissolved in THF (0.2 wt %) and filtered through 0.45 μm filters before injection into the GPC column. Chromatographs were obtained using both refractive index and fluorescence detectors; in the latter case, the monochromator was set to detect fluorescence at 550 nm.

UV−vis absorption measurements were made using a Hewlett-Packard 8452A diode-array spectrophotometer with 2 nm resolution. Quantitative analysis was achieved by obtaining spectra of both the labeled polymer and the perylene derivative in $CHCl_3$ solutions over a range of concentrations. In both cases, the optical density at the absorption maximum was plotted versus concentration, and an extinction coefficient, ϵ_{max}, was determined from the slope of the linear function:

$$\epsilon_{max} = A_{max}/cl \tag{1}$$

where A is the absorbance, or optical density, at the absorption maximum, c is the solution concentration (g mL^{-1} or mol L^{-1}), and l is the path length (1 cm). The mole fraction of perylene in the labeled polymer, y_d, was determined from the ratio of extinction coefficients for the polymer, $\epsilon_{p,max}$, and the perylene dye, $\epsilon_{d,max}$ (both in units of L mol^{-1} cm^{-1}):

$$y_d = \epsilon_{p,max}/\epsilon_{d,max} \tag{2}$$

Fluorescence Measurements. Toluene solutions of perylene-labeled SEBS and the perylene derivative **1**, with concentrations of 1.4 mg/mL and 2.0 × 10^{-7} M, respectively, were prepared. Prior to all measurements, the solutions were degassed by bubbling with N_2 in a septum-sealed quartz tube. A thin film of the labeled polymer was prepared on a small quartz plate (1 cm × 2 cm) by casting from CCl_4 solution. The thickness of the film was determined from the optical density to be ~70 μm. The film was also degassed prior to fluorescence measurements, using flowing N_2 in a sealed quartz tube.

Excitation and emission spectra of the film and solutions were obtained using a SPEX Fluorolog 2 spectrometer with double-grating monochromators, a red-sensitive photomultiplier, and a photon-counting detector. For the film sample, the slit widths were set at 0.5 mm, while for the solution samples 1.0 mm slit widths were used. A right-angle geometry setting was used for data collection, and all spectra were recorded in sample over reference mode (S/R).

Chart 2

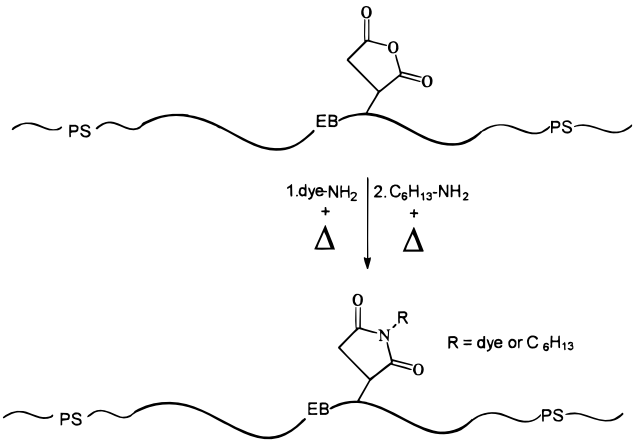

Dynamic fluorescence measurements were carried out by the time-correlated single photon counting technique, using a pulsed lamp as the excitation source. For λ_{ex} = 450 nm (solutions) and λ_{ex} = 500 nm (film), stray light from the excitation source was filtered using 500 and 550 nm cutoff filters, respectively. Further information on excitation and emission settings for the experiments is described in the Results and Discussion section. Data were collected at room temperature, with a 90° angle between the detector and excitation source. Single photon counting experiments were run until 5000 counts had been collected in the maximum channel.

The fluorescence decay profiles were fit using single-, double-, and triple-exponential functions:

$$I(t) = \sum_{i=1}^{n} A_i \exp(-t/\tau_i) \tag{3}$$

where n = 1, 2, or 3. In the case of a double-exponential fit, the short and long lifetimes are represented τ_{short} and τ_{long}, with preexponential factors A_{short} and A_{long}. In all cases, data were fit from 1 to 5 channels after the maximum channel (5 × 10^3 counts) to the region of the profile in which intensity had decayed to 10^1 counts.

Results and Discussion

Characterization of Perylene-Labeled SEBS: FTIR, GPC, and UV−vis Results. In the application of dyes as fluorescent labels for polymer systems, the concentration of dye is generally kept extremely low, so as not to affect the physical properties of the polymer under study. Chart 2 outlines the general strategy for attaching fluorescent dyes to maleated SEBS, where PS is polystyrene and EB is a random copolymer of ethylene and butylene (Note: the chart does not represent the degree of maleation; there are in fact about 13 anhydride groups per EB block.) In the present case, the aim of the post-polymerization reaction was to attach only one dye molecule per polymer chain. This procedure was carried out in two steps: first, the maleated polymer was reacted with a stoichiometric quantity of dye **1**, relative to the number of polymer chains; next, the remaining anhydride groups on the polymer were reacted with an excess of hexylamine. It was assumed that the low-molecular-weight hydrocarbons will not greatly affect the properties of the polymer, especially since the initial quantity of anhydride groups on the chain is low (2 wt %).

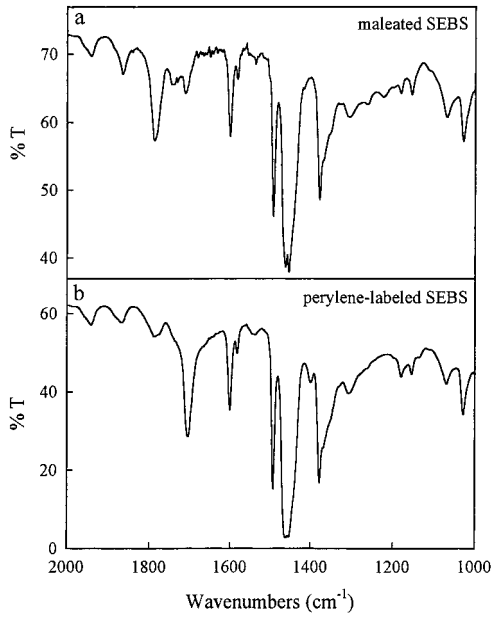

Figure 1. Fourier transform infrared spectra of (a) maleated SEBS copolymer and (b) perylene-labeled SEBS copolymer. Both spectra were obtained after heating the films at 120 °C under vacuum for 2 h. The anhydride bands (1866 and 1785 cm^{-1}) from the maleated sample (a) have mostly disappeared in the dye-labeled polymer (b); the latter sample shows a sharp band at 1705 cm^{-1}, attributed to imide links between the dye and polymer.

FTIR spectra of the SEBS copolymer, before and after the labeling procedure, are shown in Figure 1. Before labeling, the maleated polymer shows distinct bands at 1866 and 1785 cm^{-1}, attributed to succinic anhydride functionalities (Figure 1a). Following reaction with the perylene dye, the intensity of succinic anhydride bands decreases dramatically, in favor of a single sharp band at 1705 cm^{-1} (Figure 1b). These results are consistent with the nearly complete conversion of anhydride groups into imide linkages between the dye, or the low-molecular-weight hydrocarbons, and the polymer.[23]

To confirm that all of the dye in the perylene-labeled sample was covalently linked to the polymer, the polymer product was dissolved in tetrahydofuran (THF) and injected into a gel permeation chromatography column. The eluted sample was detected using both a refractive index detector, which is sensitive to the presence of the polymer in solution, and a fluorescence detector, which is sensitive to the presence of the perylene dye. The chromatographs obtained using these different detectors both showed a single peak at identical elution volumes, indicating that the dye was, in fact, attached to the polymer and that no residual, unattached perylene derivative was present in the sample.

The degree of dye labeling was determined from quantitative UV−vis analysis of the perylene-labeled SEBS and the unattached perylene derivative **1**, in solutions of chloroform at various concentrations. For the labeled polymer, three solutions between 1.3 and 6.5 mg/mL were found to have optical densities between 0.12 and 0.57 (path length = 1 cm) at the absorption maximum, $\lambda_{max} = 496$ nm. The resulting data were fit with a straight line passing through the origin ($r^2 = 0.99$), and the extinction coefficient, $\epsilon_{p,496} = 87$ cm^3 g^{-1} cm^{-1}, was obtained from the slope. Considering $M_n = 84\,400$ g mol^{-1} for the polymer, the extinction coefficient was also expressed in terms of the number of polymer chains in solution, $\epsilon_{p,496} = 7400$ L mol^{-1} cm^{-1}. In the case of the unattached dye, the absorbance maximum showed a slight red shift with respect to the labeled polymer, $\lambda_{max} = 500$ nm; the extinction coefficient at the maximum was determined to be $\epsilon_{d,500} = 33\,000$ L mol^{-1} cm^{-1}. Assuming that the extinction coefficient of the dye in chloroform is not significantly affected by chemical attachment to the polymer, the values $\epsilon_{p,496}$ and $\epsilon_{d,500}$ were used to calculate the mole fraction of dye in the labeled polymer, $y_d = 0.23$ (eq 2). This suggests that the perylene-labeled SEBS contains an average of one dye molecule per five polymer chains. This is an even lower degree of labeling than expected, on the basis of the stoichiometry of added dye. However, the result is not really surprising, when we consider that the kinetics of polymer functionalization are generally slow, due to large polymer molecular weights which give rise to low molar concentrations. The question of whether the dye is randomly distributed throughout the polymer sample remains; we will return to this issue later on, in light of steady-state and time-resolved fluorescence data and spectroscopic evidence of dye aggregate formation.

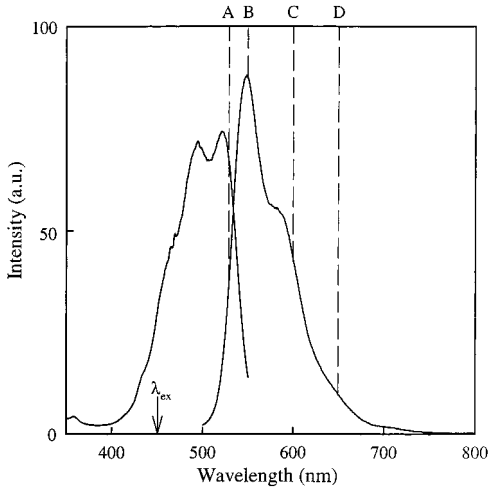

Figure 2. Excitation and emission spectra of perylene-labeled SEBS in toluene solution. For fluorescence decay experiments, $\lambda_{ex} = 450$ nm (indicated by an arrow); decay profiles were measured at $\lambda_{em} = 530$, 550, 600, and 650 nm, as indicated by the vertical dashed lines A, B, C, and D, respectively.

Spectroscopic Properties of Perylene-Labeled SEBS in Toluene Solution. Excitation and emission spectra of perylene-labeled SEBS in toluene solution ($c = 1.4$ mg/mL), obtained at $\lambda_{em} = 570$ nm and $\lambda_{ex} = 480$ nm, respectively, are shown in Figure 2. Also shown in the figure are excitation and emission wavelengths for fluorescence decay measurements of the same solution. As indicated by an arrow, all fluorescence decay data were collected using an excitation wavelength of $\lambda_{ex} = 450$ nm; the vertical dashed lines indicate the four different emission wavelengths at which the decay profiles were measured, $\lambda_{em} = 530$, 550, 600, and 650 nm.

Figure 3 shows the fluorescence decay profile for the perylene-labeled SEBS solution, measured at $\lambda_{em} = 600$ nm. When the data are fit to a single-exponential function (Figure 3a), nonrandom fluctuations are observed in the weighted residuals and the autocorrelation function, and a high χ^2 value ($\chi^2 = 3.1$) is obtained for the fit. This suggests that the profile is not well represented by a single-exponential function, although the resulting lifetime, $\tau = 4.9$ ns, is in the neighborhood

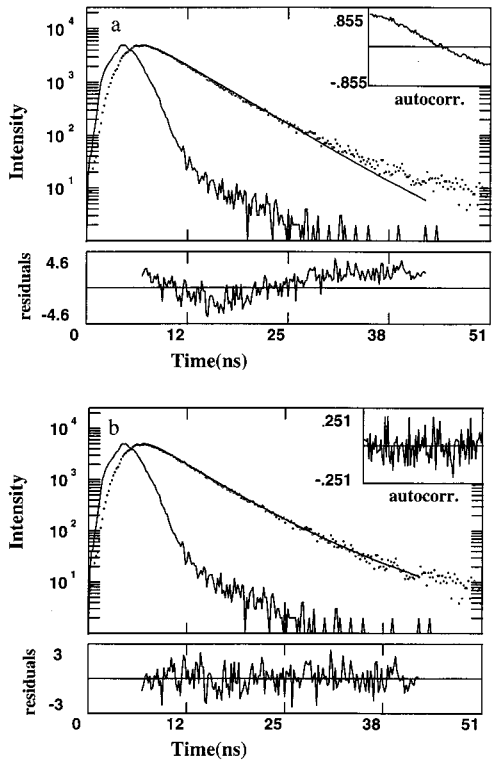

Figure 3. Fluorescence decay profile for perylene-labeled SEBS in toluene solution, $\lambda_{ex} = 450$ nm and $\lambda_{em} = 600$ nm. (a) Single-exponential fit: $\chi^2 = 3.1$, $\tau = 4.9$ ns. (b) Double-exponential fit: $\chi^2 = 1.0$, $\tau_{short} = 4.4$ ns, $\tau_{long} = 9.2$ ns, $A_{short}/A_{long} = 15.9$, $\tau_{ave} = 4.7$ ns.

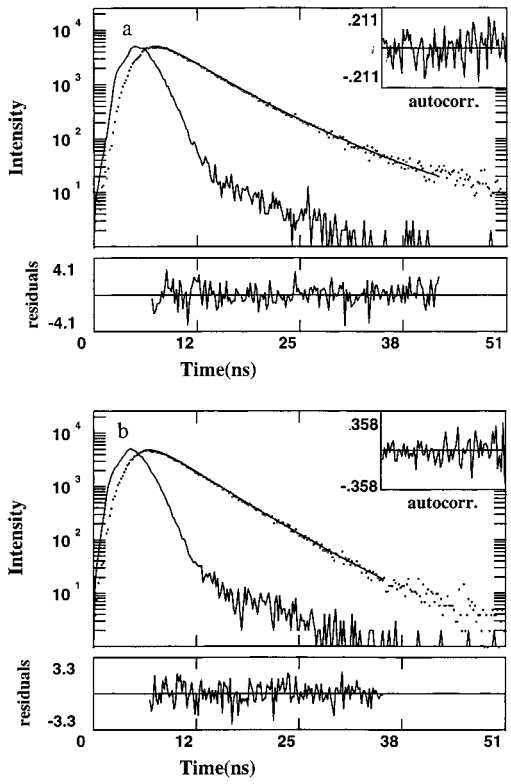

Figure 4. Comparison of fluorescence decay profiles for perylene-labeled SEBS in toluene solution, $\lambda_{ex} = 450$ nm, measured at $\lambda_{em} = 650$ and 550 nm. Both profiles are fit to a double-exponential function, with τ_{long} fixed at 9.2 ns. (a) $\lambda_{em} = 650$ nm: $\chi^2 = 1.2$, $\tau_{short} = 4.4$ ns, $A_{short}/A_{long} = 11.0$, $\tau_{ave} = 4.8$ ns. (b) $\lambda_{em} = 550$ nm: $\chi^2 = 0.9$, $\tau_{short} = 4.4$ ns, $A_{short}/A_{long} = 65.3$, $\tau_{ave} = 4.5$ ns.

of the literature value for unfunctionalized perylene in toluene solution ($\tau = 5.5$ ns).[24] A greatly improved fit is obtained using a double-exponential function (Figure 3b), as shown by evenly distributed residuals and autocorrelation data, and a low χ^2 value ($\chi^2 = 1.0$). The resulting short and long lifetimes are $\tau_{short} = 4.4$ ns and $\tau_{long} = 9.2$ ns, with a ratio of preexponential factors $A_{short}/A_{long} = 15.9$. The average lifetime of the decay is $\tau_{ave} = 4.7$ ns. It is important to point out that a good double-exponential fit does not necessarily mean that the quantities τ_{short} and τ_{long} have physical significance. For example, a single emitting species may exhibit nonexponential decay by mechanisms such as energy transfer or solvent relaxation that can be approximately represented by sums of two or more exponentials.[25] Further evidence is therefore required to determine whether τ_{short} and τ_{long} can be attributed to identifiable fluorescent species.

As indicated by the vertical dashed lines in Figure 2, decay profiles were measured at different emission wavelengths, and two of these ($\lambda_{em} = 650$ and 550 nm) are compared in Figure 4. Careful inspection of the profiles reveals that the fluorescent emission at $\lambda_{em} = 650$ nm (Figure 4a) decays more slowly than the emission at $\lambda_{em} = 550$ nm (Figure 4b). Both profiles in Figure 4 are fit using a double-exponential function, with the longer lifetime fixed at the value obtained for $\lambda_{em} = 600$ nm ($\tau_{long} = 9.2$ ns). In both cases, the residuals and autocorrelation function indicate a good fit, with χ^2 values close to 1 ($\chi^2 = 1.2$ for $\lambda_{em} = 650$ nm and $\chi^2 = 0.9$ for $\lambda_{em} = 550$ nm). More importantly, with τ_{long} fixed at 9.2 ns, the short lifetime, $\tau_{short} = 4.4$ ns, is recovered in both cases, such that short and long lifetimes are identical for $\lambda_{em} = 550$, 600, and 650 nm. However, while τ_{short} and τ_{long} remain constant, the average lifetime, τ_{ave}, of fluorescence decay shows a small but systematic increase from 4.5 to 4.8 ns as the wavelength increases from 550 to 650 nm, due to a decrease in the ratio of preexponential factors, A_{short}/A_{long}. A similar analysis was carried out for $\lambda_{em} = 530$ nm (not shown), and values obtained from the double-exponential fit obey the same trend (Table 1). Since $\tau_{short} = 4.4$ ns and $\tau_{long} = 9.2$ ns are recovered over a range of wavelengths, despite systematic changes in the average lifetime, it appears that these two lifetimes do indeed have physical significance and can therefore be attributed to different emitting species present in the sample. From the behavior of the ratio A_{short}/A_{long}, we also conclude that the contribution of the longer-lived species is greater at higher wavelengths, at least in the range $\lambda_{em} = 530-650$ nm. At this point, we tentatively assign the longer lifetime, $\tau_{long} = 9.2$ ns, to aggregates of dye molecules within the solution of labeled polymer, so that $\tau_{short} = 4.4$ ns is ascribed to individual, nonaggregated dye labels (unimers).

Table 1. Average Lifetimes and Preexponential Ratios for Fluorescence Decay Profiles, Determined at Different Emission Wavelengths λ_{em}

λ_{em} (nm)	perylene-labeled SEBS solution A_{short}/A_{long} ($\tau_{short} =$ 4.4 ns, $\tau_{long} = 9.2$ ns)	perylene-labeled SEBS solution τ_{ave} (ns)	perylene dye **1** solution τ_{ave} (ns)	perylene-labeled SEBS film τ_{ave} (ns)
530	63.4	4.5		
550	65.3	4.5	4.3	
600	15.9	4.7	4.3	7.1
650	11.0	4.8		
710				9.3

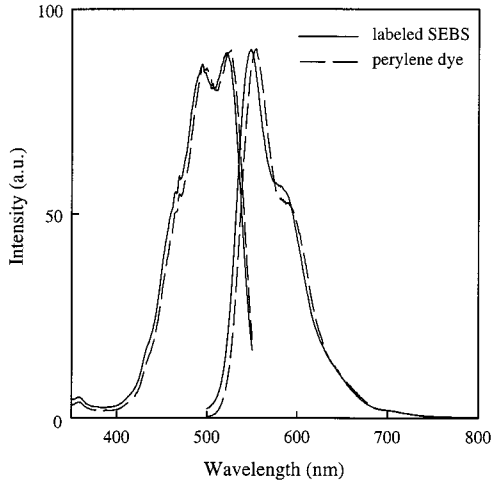

Figure 5. Comparison of excitation and emission spectra, for perylene-labeled SEBS (solid line) and perylene model dye **1** (dashed line) in toluene solution. The spectra have been normalized to the emission maxima.

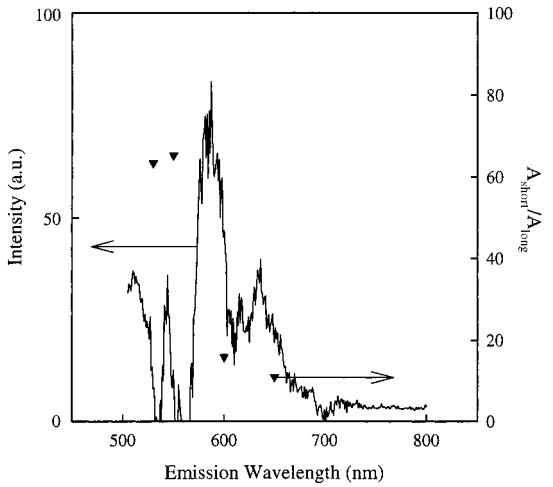

Figure 6. Difference in the normalized emission spectra from Figure 5 (corrected for wavelength shift). The resulting emission spectrum is attributed to dye aggregates within the labeled polymer and is compared with A_{short}/A_{long} values from fluorescence decay measurements of the labeled polymer (Table 1).

Normalized excitation and emission spectra of perylene-labeled SEBS and the unattached perylene derivative **1** in toluene solution are compared in Figure 5. The spectra of the perylene derivative were obtained in an extremely dilute solution ($c = 2.0 \times 10^{-7}$ M) to prevent the formation of dye aggregates. The spectra are found to be quite similar, although a blue shift of 5 nm is observed when the dye is attached to the polymer. As well, the emission shoulder at 580 nm is found to be more pronounced in the case of the labeled polymer.

The difference in the emission spectra of the labeled polymer, I_p, and the unattached dye, I_d, after correction for the blue shift is shown in Figure 6. Since the dilute solution of unattached dye is not believed to contain any aggregates (a supposition that will be investigated more closely later on), the resulting spectrum ($I_p - I_d$) is attributed to the emission of dye aggregates in the perylene-labeled polymer solution. Superimposed on the emission spectrum are the ratios A_{short}/A_{long}, determined from fluorescence decay profiles. It is found that a sharp drop in A_{short}/A_{long}, indicating a sudden increase in the contribution of the longer-lived species, corresponds with the onset of aggregate emission. This provides further evidence that the longer lifetime, $\tau_{long} = 9.2$ ns, can be attributed to the fluorescence decay of dye aggregates in the solution of perylene-labeled SEBS. It should be noted that the ratio A_{short}/A_{long} at a given wavelength is related not only to the intensity of the aggregate emission spectrum but also to the intensity of unimer emission. This explains why A_{short}/A_{long} is found to decrease slightly between $\lambda_{em} = 600$ and 650 nm, even though the emission of aggregates becomes less intense; in the same range, the fluorescence emission of unimers, represented by the dashed spectrum in Figure 5, decreases significantly, such that the overall contribution of aggregate emission increases.

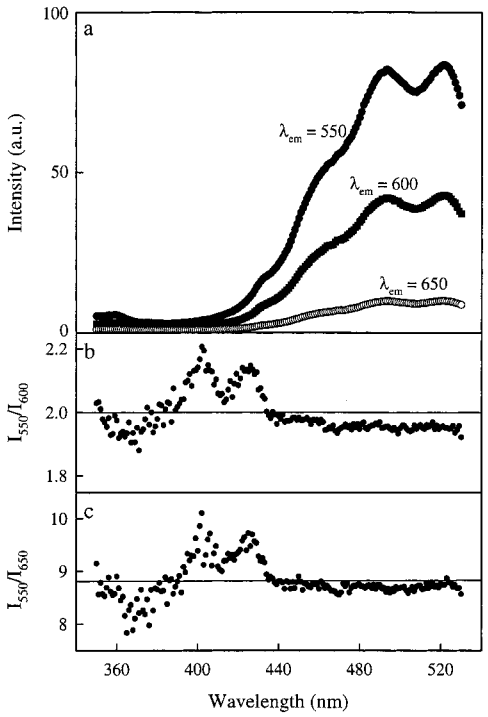

Figure 7. (a) Comparison of excitation spectra of perylene-labeled SEBS in toluene solution, obtained at $\lambda_{em} = 550$, 600, and 650 nm. (b) Ratios of the spectra obtained at $\lambda_{em} = 550$ and 600 nm (I_{550}/I_{600}); (c) $\lambda_{em} = 550$ and 650 nm (I_{550}/I_{650}).

Excitation spectra of the perylene-labeled SEBS solution were also obtained at three different emission wavelengths, $\lambda_{em} = 550$, 600, and 650 nm; one of these, $\lambda_{em} = 550$ nm, is outside the region of aggregate emission (Figure 6), while the other two emission wavelengths, $\lambda_{em} = 600$ and 650 nm, fall within the region where aggregate and unimer emission overlap. The three excitation spectra appear to be very similar, apart from intensity differences (Figure 7a); however, the ratios of the spectra, I_{550}/I_{600} and I_{550}/I_{650} (Figure 7, b and c, respectively), show obvious nonrandom fluctuations, revealing subtle differences in excitation spectra that are collected inside and outside the region of aggregate emission. This suggests that the aggregates exist in the ground state and do not form after the unimers are excited, as in the case of excimers or exciplexes. The ratio I_{600}/I_{650} (not shown) indicates less marked differences in the two excitation spectra collected within the region of aggregate emission, although fluctuations about the average are not entirely random; this is not an unexpected result, as the relative contribution of the two species will also change in the region where aggregate and unimer emission overlap.

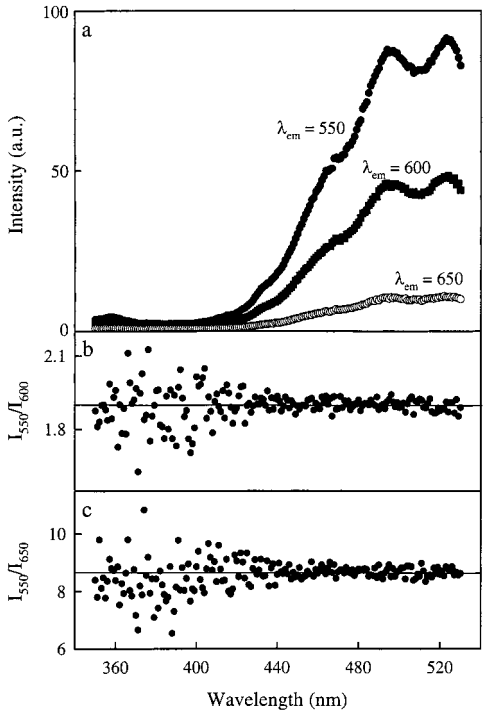

Figure 8. (a) Comparison of excitation spectra of perylene model dye **1** in toluene solution, obtained at λ_{em} = 550, 600, and 650 nm. (b) Ratios of the spectra obtained at λ_{em} = 550 and 600 nm (I_{550}/I_{600}); (c) λ_{em} = 550 and 650 nm (I_{550}/I_{650}).

Excitation spectra of the dilute solution of perylene derivative **1** were also obtained at the three emission wavelengths, λ_{em} = 550, 600, and 650 nm. In this case, the ratios I_{550}/I_{600} and I_{550}/I_{650} show only random fluctuations about average values, suggesting that the excitation spectra are independent of λ_{em} (Figure 8). This provides further evidence for the assumption that ground-state aggregates are not present in the solution of unattached dye molecules and seem to be related to the chemical attachment of perylene dye to the polymer chain. This is not believed to be an effect of global dye concentration, as the overall concentration of perylene derivative in the labeled polymer solution is also extremely dilute (3.3×10^{-6} M). Rather, chemical attachment to the polymer chain may increase the local concentration of dye molecules, promoting the formation of aggregates. Since both block types in the SEBS copolymer are completely soluble in toluene, micelle formation would not be a likely mechanism for dye localization, especially at such a low concentration of polymer chains (1.7×10^{-5} M). A more plausible explanation is that the dye molecules distribute themselves nonrandomly during the labeling reaction, such that a certain number of polymer chains contain more than one dye label. Intracoil complexes could then form by a mechanism of chain looping within the labeled olefin block. Although the exact nature of these complexes is unknown, the formation of aggregates larger than dimers would not be expected at such a low degree of dye labeling.

It was also of interest to determine the lifetime of the perylene derivative **1** in toluene solution, for comparison with the short lifetime τ_{short} in the solution of labeled polymer. Excitation and emission wavelengths for fluorescence decay experiments (λ_{ex} = 450 nm; λ_{em} = 550 and 600 nm) are indicated in Figure 9, superimposed on fluorescence spectra of the perylene dye solution. The fluorescence decay profile for λ_{em} = 550 nm (not shown)

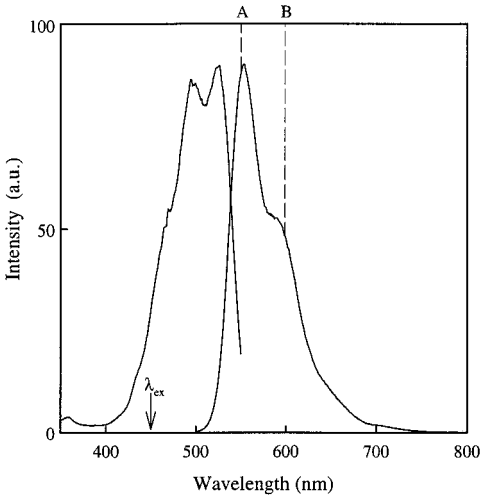

Figure 9. Excitation and emission spectra of perylene model dye **1** in toluene solution. For fluorescence decay experiments, λ_{ex} = 450 nm (indicated by an arrow); decay profiles were measured at λ_{em} = 550 and 600 nm, as indicated by the vertical dashed lines A and B, respectively.

is found to show slight deviations from single-exponential behavior ($\chi^2 = 1.3$), although these are not as severe as those observed in the labeled polymer solution. The lifetime from the single-exponential function, τ = 4.4 ns, is identical to τ_{short} in the labeled polymer, suggesting that τ_{short} can indeed be attributed to fluorescence of the unimer. A somewhat improved fit is obtained using the double-exponential function, resulting in an average lifetime τ_{ave} = 4.3 ns. Since aggregates are not thought to be present in the unattached dye solution, the physical meaning, if any, of the short and long components is unclear. In fact, the percent contribution of the longer lifetime, determined from

$$\text{emission \%}_{long} = 100x\left[\frac{A_{long}\tau_{long}}{A_{long}\tau_{long} + A_{short}\tau_{short}}\right] \quad (4)$$

is only 1.5%. This suggests that $A_{long}\tau_{long}$ is simply a correction term that cannot be ascribed to any emitting population. The fluorescence decay profile measured at λ_{em} = 600 nm (not shown) was also fit to a double-exponential function, and the average lifetime, τ_{ave} = 4.3 ns, was found to be identical to that determined for λ_{em} = 550 nm (Table 1). This is in contrast to the case of the perylene-labeled polymer, where τ_{ave} shows a definite λ_{em} dependence. This result, together with the results of Figures 7 and 8, strongly suggests an overlap of aggregate and unimer populations in the labeled polymer that is not present in a dilute solution of the unattached dye.

Finally, the present decay data allow some qualitative conclusions to be made on the kinetics of aggregate−unimer exchange. If a rapid equilibrium between populations were present, it can be shown that τ_{short} and τ_{long} would not be equal to the lifetimes of unimers and aggregates, respectively, but would be complicated functions of both lifetimes and the rate constants of association/dissociation.[26] However, we have found τ_{short} for the labeled polymer and τ for the unattached dye to be identical (or nearly identical, in the case of a double-exponential fit) and thus conclude that aggregate and unimer populations are not in dynamic equilibrium. The term "aggregate", implying kinetically frozen associates of dye molecules, therefore seems appropriate in the present case.

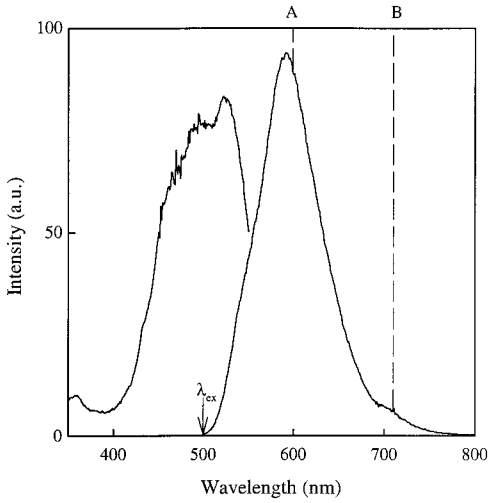

Figure 10. Excitation and emission spectra of a solid film of perylene-labeled SEBS. For fluorescence decay experiments, $\lambda_{ex} = 500$ nm (indicated by an arrow); decay profiles were measured at $\lambda_{em} = 600$ and 710 nm, as indicated by the vertical dashed lines A and B, respectively.

Spectroscopic Properties of a Perylene-Labeled SEBS Film. Excitation and emission spectra of a thin film (~70 μm) of the perylene-labeled SEBS sample (Figure 10), measured at $\lambda_{em} = 570$ nm and $\lambda_{ex} = 480$ nm, respectively, are found to be dramatically different from spectra of the labeled polymer in toluene solution obtained under the same collection conditions (Figure 2). Most notably, the emission maximum at 550 nm (Figure 2) is no longer present; instead, a single, broad maximum, centered at 590 nm, is observed in the solid film. This marked decrease in emission at 550 nm is not attributed to autoabsorption within the polymer film, as the optical density of the film at this wavelength ($A_{550} = 0.25$) is below the range where such a prominent effect would be observed. To confirm this, an even thinner film of the labeled polymer was prepared (thickness ~16 μm, $A_{550} = 0.05$); steady-state fluorescence measurements of the thinner film showed the same broad peak at 590 nm, indicating that the observed differences in solution and solid-state emission spectra are not related to differences in optical density.

It is further noted that the emission maximum in the films (590 nm) corresponds very closely to the emission maximum of dye aggregates in solution (Figure 6). This suggests that changes in the fluorescence spectra are related to a significant increase in the number of aggregates in the solid state, probably due to microphase separation during polymer film formation. Although, as has already been discussed, the occurrence of microphase separation is not likely in an organic solvent such as toluene, the gradual removal of solvent allows the system to approach its bulk morphology. Since the two block types are immiscible in the bulk, solvent removal eventually leads to microphase separation of the perylene-labeled polyolefin, confining the labeled blocks to domains of molecular dimensions and increasing local dye concentrations. An increase in the local concentration of perylene within the polyolefin microdomains results in a decrease in the average distance between labels, allowing a greater number of aggregates to form.

Also shown in Figure 10 are excitation and emission conditions for fluorescence decay measurements of the 0.75 μm solid film ($\lambda_{ex} = 500$ nm; $\lambda_{em} = 600$ and 710 nm). Assuming that some unimer will contribute to fluorescence of the solid film, the fluorescence decay profile at $\lambda_{em} = 600$ nm is fit using a double-exponential function with τ_{short} fixed at 4.4 ns (Figure 11a). Compared with the solution of labeled polymer, the decay of the film is found to be slow, indicating a greater contribution from the longer lifetime. The imperfect fit ($\chi^2 = 1.4$) may be due to a distribution of aggregate lifetimes within the solid film. Such a distribution could be explained by various aggregate sizes within the concentrated environment of the microdomains. It is also possible that the highly viscous medium of the polyolefin prevents the dyes from reaching the most favorable orientation with respect to their dimer counterparts, forcing them to adopt a distribution of orientations with different emission properties. In any case, it is found that the distribution of lifetimes can be better represented using a triple-exponential function (Figure 11b), with the unimer lifetime still fixed at $\tau_{short} = 4.4$ ns. The resulting fit is acceptable ($\chi^2 = 1.1$), with random behavior in the weighted residuals and the autocorrelation function, and gives an average lifetime of $\tau_{ave} = 7.1$ ns. As the two longer lifetimes are meant to represent a larger distribution of exponentials, they are not believed to have physical significance individually. However, the lifetimes and preexponential factors from the triple-exponential fit can be used to calculate the fractional contribution of unimer fluorescence, f_{short}, according to the following expression:

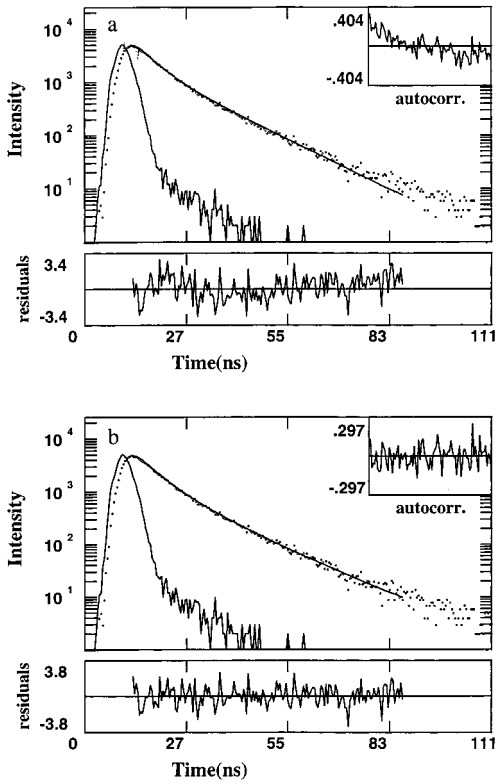

Figure 11. Fluorescence decay profile for a solid film of perylene-labeled SEBS, $\lambda_{ex} = 500$ nm and $\lambda_{em} = 600$ nm. (a) Double-exponential fit (τ_{short} fixed at 4.4 ns): $\chi^2 = 1.4$, $\tau_{long} = 12.7$ ns, $A_{short}/A_{long} = 2.4$. (b) Triple-exponential fit (τ_{short} fixed at 4.4 ns): $\chi^2 = 1.1$, $f_{short} = 0.36$, $\tau_{ave} = 7.1$ ns.

$$f_{short} = \frac{A_{short}\tau_{short}}{\sum_i A_i \tau_i} \qquad (5)$$

Table 2. Fractional Contribution of Unimer Emission to Fluorescence of Perylene-Labeled SEBS at Different Emission Wavelengths λ_{em}

λ_{em} (nm)	perylene-labeled SEBS solution f_{short}	perylene-labeled SEBS film f_{short}
530	0.97	
550	0.97	
600	0.88	0.36
650	0.84	
710		0.10

From the decay profile, we thus calculate the fractional contribution of unimer fluorescence in the solid film to be $f_{short} = 0.36$ at $\lambda_{em} = 600$ nm; this quantity is related to the weight fraction of unimers through the quantum yields of the unimer and each of the aggregate species. f_{short} values have also been calculated for the perylene-labeled polymer in toluene solution (Table 2) and are found to range from 0.97 outside the principal region of aggregate emission ($\lambda_{em} = 530$ nm) to 0.84 at $\lambda_{em} = 650$ nm. This comparison of f_{short} values in solution and film provides further evidence that the amount of aggregation is much higher in the polymer film.

A similar situation is found for $\lambda_{em} = 710$ nm, and a greatly improved fit of the decay data is again obtained when three, rather than two, exponentials are used (not shown). In the case of a triple-exponential fit with τ_{short} fixed at 4.4 ns, $f_{short} = 0.10$ and $\tau_{ave} = 9.7$ ns at this emission wavelength. This is analogous to the behavior of the labeled polymer solution, where the unimer contribution is found to decrease at higher emission wavelengths. In the case of the polymer film, however, the overall contribution of aggregates is much more significant, resulting in longer decay times (7−10 ns) with more dramatic wavelength dependence.

Conclusions

Fluorescence decay profiles of an SEBS block copolymer, labeled with perylene derivative **1** (Chart 1), were obtained at different emission wavelengths in toluene solution and in a thin film. For the solution of labeled polymer, a double-exponential function was used to fit fluorescence decay profiles, and the same two lifetimes, $\tau_{short} = 4.4$ ns and $\tau_{long} = 9.2$ ns, were recovered at different emission wavelengths; the contribution of the longer lifetime was found to increase with increasing wavelength. This behavior is attributed to the formation of dye aggregates in the labeled polymer, and short and long lifetimes are assigned to unimers and aggregates, respectively. Due to the low degree of labeling, the aggregates are believed to be dimers of the perylene labels. The assignment of $\tau_{long} = 9.2$ ns to the aggregates is supported by steady-state fluorescence data, as the onset of aggregate emission corresponds to a sharp decrease in the ratio of preexponential factors, A_{short}/A_{long}. As well, the lifetime of the unattached perylene dye is almost identical to τ_{short}, suggesting that unimers and aggregates are not in dynamic equilibrium. In the case of the labeled polymer, the observed dependence of the excitation spectra on emission wavelength indicates that the aggregates exist in the ground state.

Fluorescence spectra and decay data from a thin film of the labeled polymer indicate that the amount of aggregation in the solid state is greater than that in solution; this is likely due to local concentration effects, arising from microphase separation of the labeled block. The fractional contribution of unimer fluorescence in the polymer film ($f_{short} = 0.36-0.10$) is therefore much smaller than that in solution ($f_{short} = 0.97-0.84$), resulting in longer fluorescence lifetimes in the solid state. Since a triple-exponential function was required to fit these decay profiles, we speculate that a distribution of dimers in different states of orientation, or a distribution of aggregate sizes, may form in the polymer film.

It should be noted that the existence of ground-state dimers, such as those found in the present system, would in no way inhibit the usefulness of this dye as a label for laser scanning confocal fluorescence microscopy (LSCFM) experiments. This is due to the low resolution of this optical microscopy technique, which is not sensitive to heterogeneities in dye concentration at the molecular level. Even if aggregates are present, the dye should appear evenly distributed throughout the labeled sample; this supposition will be investigated in future LSCFM experiments on the perylene-labeled SEBS polymer. On the other hand, the aggregation of dye labels would make energy-transfer (ET) experiments very difficult, as this technique is sensitive to local concentrations on a molecular scale and to spectroscopic differences between unimers and aggregates. From the results of the present work, it seems that the interpretation of ET experiments involving perylene labels would be particularly complicated in the solid state, where dye aggregation appears to be more prominent. However, the advantages of perylene labels (e.g., optical stability, low-energy absorption and emission) convince us that their application as molecular-level probes should not be ruled out, provided that a detailed understanding of perylene aggregation can be obtained.

Acknowledgment. The authors thank Materials and Manufacturing Ontario (MMO) for support of this research. M.M. thanks Natural Science and Engineering Research of Canada (NSERC) for funding provided by a postdoctoral fellowship. J.P.F. acknowledges the support of FCT-PRAXIS XXI.

References and Notes

(1) Zollinger, H. *Color Chemistry: Synthesis, Properties and Applications of Organic Dyes and Pigments*, 2nd ed.; VCH: Weinheim, 1991.
(2) Reisfeld, R.; Brusilovsky, D.; Eyal, M.; Miron, E.; Burshtein, Z.; Ivri, J. *Chem. Phys. Lett.* **1989**, *160*, 43.
(3) Reisfeld, R.; Seybold, G. *Chimia* **1990**, *44*, 295.
(4) GEC, G.B. Patent 2, 189, 502A, 1986.
(5) BASF, German Patents 3001, 857 and 3001, 858, 1980.
(6) Gregory, P. *High Technology Applications of Organic Colorants*; Plenum Press: New York, 1991.
(7) Tasch, S.; List, E. J. W.; Hochfilzer, C.; Leising, G.; Schlichting, P.; Rohr, U.; Geerts, Y.; Scherf, U.; Müllen, K. *Phys. Rev. B* **1997**, *56*, 4479.
(8) Anton, U.; Müllen, K. *Macromolecules* **1993**, *26*, 1248.
(9) Karayannidis, G.; Stamelos, D.; Bikiaris, D. *Makromol. Chem.* **1993**, *194*, 2789.
(10) Dotcheva, D.; Klapper, M.; Müllen, K. *Macromol. Chem. Phys.* **1994**, *195*, 1905.
(11) Quante, H.; Schlichting, P.; Rohr, U.; Geerts, Y.; Müllen, K. *Macromol. Chem. Phys.* **1996**, *197*, 4029.
(12) Ghassemi, H.; Hay, A. S. *Macromolecules* **1994**, *27*, 4410.
(13) (a) Harrison, W. J.; Mateer, D. L.; Tiddy, J. T. *J. Phys. Chem.* **1996**, *100*, 2310. (b) Ilich, P.; Mishra, P. K.; Macura, S.; Burghardt, T. P. *Spectrochim. Acta, Part A* **1996**, *52*, 1323. (c) Burghardt, T. P.; Lyke, J. E.; Ajtai, K. *Biophys. Chem.* **1996**, *59*, 119. (d) Dutta, A. K.; Kamada, K.; Ohta, K. *J. Photochem. Photobiol. A* **1996**, *93*, 57. (e) Maekawa, M.; Kondo, M. *Colloid Polym. Sci.* **1996**, *274*, 1145. (f) Gorduza, V.-M.; Wagner, L.; Comanita, E. *Rev. Roum. Chim.* **1995**, *40*, 759. (g) McKerrow, A. J.; Buncel, E.; Kazmaier, P. M. *Can. J. Chem.* **1995**, *73*, 1605. (h) Ford, W. E. *J. Photochem.* **1987**, *37*, 189. (i) Herz, A. H. *Adv. Colloid Interface Sci.* **1977**, *8*, 237.

(14) (a) Bilski, P.; Dabestani, R.; Chignell, C. F. *J. Photochem. Photobiol. A* **1994**, *79*, 121. (b) Chudinova, G. K.; Barachevskii, V. A. *Russ. Chem. Bull.* **1995**, *44*, 96.
(15) (a) Fujieda, T.; Ohta, K.; Wakabayashi, N.; Higuchi, S. *J. Colloid Interface Sci.* **1997**, *185*, 332. (b) Karolin, J.; Johansson, L. B.-Å; Ring, U.; Langhals, H. *Spectrochim. Acta, Part A* **1996**, *52*, 747. (c) Johansson, L. B.-Å.; Langhals, H. *Spectrochim. Acta, Part A* **1991**, *47*, 857.
(16) (a) Fukuda, K.; Nakahara, H. *Colloid Surf. A* **1995**, *102*, 57. (b) Misawa, K.; Minoshima, K.; Kobayashi, T. *J. Raman Spectrosc.* **1995**, *26*, 553. (c) Kajikawa, K.; Anzai, T.; Takezoe, H.; Fukuda, A. *Thin Solid Films* **1994**, *243*, 587. (d) Vitukhnovsky, A. G.; Sluch, M. I.; Warren, J. G.; Petty, M. C. *Chem. Phys. Lett.* **1991**, *184*, 235.
(17) De Rossi, U.; Daehne, S.; Reisfeld, R. *Chem. Phys. Lett.* **1996**, *251*, 259.
(18) (a) Lenhard, J. R.; Hein, B. R. *J. Phys. Chem.* **1996**, *100*, 17287. (b) Nüesch, F.; Grätzel, M. *Chem. Phys.* **1995**, *193*, 1. (c) Itoh, K.; Chiyokawa, Y.; Nakao, M.; Honda, K. *J. Am. Chem. Soc.* **1984**, *106*, 1620.
(19) Ghassemi, H.; Zhu, J. H. *J. Polym. Sci.* **1995**, *33*, 1633.
(20) Wang, Y. *Chem. Phys. Lett.* **1986**, *126*, 209.
(21) (a) Frackowiak, D.; Goc, J.; Malak, H.; Planner, A.; Ptak, A.; Zelent, B. *J. Photochem. Photobiol. A* **1996**, *94*, 43. (b) Otsuki, S.; Adachi, K. *Polym. J.* **1995**, *27*, 655. (c) Gvishi, R.; He, G. S.; Prasad, P. N.; Narang, U.; Li, M.; Bright, F. V.; Reinhardt, B. A.; Bhatt, J. C.; Dillard, A. G. *App. Spectrosc.* **1995**, *49*, 834. (d) Schoondorp, M. A.; Schouten, A. J.; Hulshof, J. B. E.; Schudde, E. P.; Feringa, B. L. *Recl. Trav. Chim. Pays-Bas* **1994**, *113*, 250. (e) Law, K. Y.; Loutfy, R. O. *Macromolecules* **1981**, *14*, 587.
(22) Nagao, Y.; Abe, Y.; Misono, T. *Dyes Pigments* **1991**, *16*, 19.
(23) As the IR bands for amide and imide linkages are quite similar, we cannot rule out the possibility that some of the former are present; however, these are considered to be extremely unlikely, considering the reaction temperature and excess of hexylamine that was used.
(24) Ware, W. R. *J. Phys. Chem.* **1962**, *66*, 455.
(25) Lakowicz, J. R. *Principles of Fluorescence Spectroscopy*; Plenum Press: New York, 1983.
(26) Birks, J. B. *Photophysics of Aromatic Molecules*; Wiley-International: London, 1970.

MA990332S